Crystal Structure of Human Complement Protein C8γ at 1.2 Å Resolution Reveals a Lipocalin Fold and a Distinct Ligand Binding Site[†,‡]

Eric Ortlund,[#] Chasta L. Parker,[#,$] Steven F. Schreck,[#] Steve Ginell,[§] Wladek Minor,[||] James M. Sodetz,[#,⊥] and Lukasz Lebioda*[,#]

Department of Chemistry and Biochemistry and the School of Medicine, University of South Carolina, Columbia, South Carolina 29208, Department of Molecular Physiology and Biological Physics, University of Virginia, Charlottesville, Virginia 22908, and Structural Biology Center, Argonne National Laboratory, Argonne, Illinois 60439

Received February 18, 2002; Revised Manuscript Received April 3, 2002

ABSTRACT: C8γ is a 22-kDa subunit of human C8, which is one of five components of the cytolytic membrane attack complex of complement (MAC). C8γ is disulfide-linked to a C8α subunit that is noncovalently associated with a C8β chain. In the present study, the three-dimensional structure of recombinant C8γ was determined by X-ray diffraction to 1.2 Å resolution. The structure displays a typical lipocalin fold forming a calyx with a distinct binding pocket that is indicative of a ligand-binding function for C8γ. When compared to other lipocalins, the overall structure is most similar to neutrophil gelatinase associated lipocalin (NGAL), a protein released from granules of activated neutrophils. Notable differences include a much deeper binding pocket in C8γ as well as variation in the identity and position of residues lining the pocket. In C8γ, these residues allow ligand access to a large hydrophobic cavity at the base of the calyx, whereas corresponding residues in NGAL restrict access. This suggests the natural ligands for C8γ and NGAL are significantly different in size. Cys[40] in C8γ, which forms the disulfide bond to C8α, is located in a partially disordered loop (loop 1, residues 38−52) near the opening of the calyx. Access to the calyx may be regulated by movement of this loop in response to conformational changes in C8α during MAC formation.

Human C8γ is a subunit of the eighth component of complement (C8), which is one of five components (C5b, C6, C7, C8, C9) that interact to form the cytolytic membrane attack complex of complement, or MAC[1] (*1*, *2*). C8 is composed of an α (M_r = 64 000), β (M_r = 64 000), and γ (M_r = 22 000) subunit. These subunits are produced from different genes and are secreted in the form of a disulfide-linked C8α−γ dimer that is noncovalently associated with C8β (*3*). Studies of the individual subunits have provided considerable insight into the role of C8α and C8β in the formation and function of the MAC (*4*−*9*). By contrast, little is known about the role of C8γ (reviewed in ref *10*). C8γ is not required for the synthesis and secretion of C8α; C8α can be expressed independently as a recombinant protein. Binding between C8α−γ and C8β is likewise not dependent on C8γ; purified C8α and C8β can form a noncovalent complex in the absence of C8γ. This dimer exhibits C8-like activity; therefore, C8γ is not essential for incorporation of C8 into the MAC, nor is it required for expression of MAC cytolytic activity. A major goal of the present study was to gain further insight into the function of C8γ by determining its three-dimensional structure.

C8γ was initially identified as a lipocalin based on its sequence and genomic organization (*11*, *12*). Within the complement system, it has the distinction of being the only lipocalin, and among the lipocalins it is one of only a few that occur as a disulfide-linked heterodimer, i.e., C8α−γ. Lipocalins are a large family of proteins that generally bind small, hydrophobic ligands yet can also bind to large soluble macromolecules as well as cell-surface receptors (*13*, *14*). They are widely distributed in vertebrates and invertebrates and are involved in many diverse processes such as retinol transport, olfaction, pheromone binding, invertebrate coloration, and prostaglandin synthesis. The core structure, or lipocalin fold, is highly conserved among family members. It consists of an eight-stranded, antiparallel β-barrel which defines a calyx that encloses a ligand binding site (*15*). Loops linking the strands are generally short β-hairpins, except the first loop, which is often larger and located near the opening

[†] This research was supported in part by NIH Grant GM42898 awarded to J.M.S. Some instrumentation used in this research was purchased with NSF Grant BIR 9419866 and DOE Grant DE-FG-95TE00058. Use of the Argonne National Laboratory Structural Biology Center beamlines at the Advanced Photon Source was supported by the U. S. Department of Energy, Office of Science, under Contract No. W-31-109-ENG-38.

[‡] Coordinates have been deposited with the Protein Data Bank as entries 1LF7 and 1IW2 for the native structure at pH 4.0 and the native structure at pH 7.0, respectively.

* Corresponding author. Phone: 803-777-2140. Fax: 803-777-9521. E-mail: Lebioda@mail.chem.sc.edu.

[#] Department of Chemistry and Biochemistry, University of South Carolina.

[⊥] School of Medicine, University of South Carolina.

[||] University of Virginia.

[§] Argonne National Laboratory.

[$] Present Address: Department of Chemistry, Winthrop University, Rock Hill, SC 29733.

[1] Abbreviations: MAC, membrane attack complex; MAD, multiwavelength anomalous diffraction; NGAL, neutrophil gelatinase associated lipocalin; PDB, protein data bank; RBP, serum retinol binding protein.

10.1021/bi025696i CCC: $22.00
Published on Web 05/09/2002

of the calyx where it may restrict ligand access. There is a short 3_{10} helix at the N-terminus and an α-helix near the C-terminus. Residues lining the interior of the calyx and the size of the calyx vary among family members; hence, lipocalins exhibit different ligand specificities.

In the present study, we report the high-resolution crystal structure of human C8γ. Results indicate that C8γ displays a typical lipocalin fold with a distinct binding site for a small molecule. This suggests the principal function of C8γ is to bind an as yet unidentified ligand, either one that is soluble or one associated with the target membrane on which the MAC is formed.

MATERIALS AND METHODS

Purification of C8γ. Human recombinant C8γ containing a $Cys^{40} \rightarrow Gly^{40}$ mutation was produced in High Five insect cells (Invitrogen) and purified using a modification of previously published procedures (*16*). Following batch absorption of the medium and dialysis, the protein was applied to a FPLC Source 15S ion-exchange column (0.5 × 9 cm) (Amersham Biosciences) and eluted with a 0.1 to 1.5 M NaCl gradient in 20 mM sodium phosphate, pH 6.0. Fractions containing C8γ were pooled and applied to a Sephacryl S-100 column (1.6 × 60 cm) in 25 mM imidazole, 150 mM NaCl, pH 7.2. Recovered protein was pooled, concentrated, and used directly for crystallizations. Purity was assessed by SDS−PAGE, and the concentration was determined using $\epsilon_{280}^{1\%} = 17.4$ (*16*).

Crystallization. Crystals of C8γ were grown by hanging drop vapor diffusion at 4 °C from solutions containing ∼0.3−0.5 mg/mL protein in the above buffer, 28%−36% PEG 4000 and 0.1 M sodium citrate, pH 4.0. Typical crystals had dimensions of ∼0.25 × 0.15 × 0.05 mm and a tabular, orthorhombic morphology. The crystals belong to the space group $P2_12_12_1$ with unit cell dimensions $a = 42.03$ Å, $b = 58.51$ Å, $c = 71.99$ Å and one monomer per asymmetric unit (solvent content = 45%).

Heavy Atom Derivatization. To produce platinum derivatives, crystals were placed in drops containing 1 mM K_2PtCl_4 in 40% PEG 4000, 0.1 M sodium citrate, pH 7.0. After 2 days, a few dry crystals of K_2PtCl_4 were added directly to the drop, which was then allowed to sit undisturbed for two weeks. Bromide ion derivatives were obtained with a short soak (45 s) in artificial mother liquor containing 0.95 M NaBr. To obtain Xe derivatives, crystals were mounted on a loop, inverted, and placed in a Molecular Structure Corporation CRYO−Xe−SITER preequilibrated with mother liquor. The crystals were then exposed to Xe gas at a pressure of 230 psi for 10 min. After pressurization, the crystals were removed from the chamber and immediately placed in liquid N_2 to reduce Xe sublimation from the crystal.

Data Collection and Refinement. Data were collected at the Structural Biology Center beamline at the Advanced Photon Source, Argonne National Laboratory. Crystals were transferred to artificial mother liquors containing 2% glycerol as the cryoprotectant, flash-frozen in liquid N_2, and diffracted at a temperature of −160 °C. Multiwavelength anomalous dispersion (MAD) data (Br^- and Pt derivatives) were collected at four wavelengths: downstream remote ($\lambda 1$), inflection point ($\lambda 2$), peak of X-ray absorption ($\lambda 3$), and upstream remote ($\lambda 4$). Wavelengths producing the minimum

Table 1: Data Collection and Phasing Statistics

derivative	max resolution (Å)	% completeness overall	% completeness last shell	R_{sym}[a] (%)	no. of unique reflns	mosaicity (degrees)
platinum						
$\lambda 1$ (1.0721)	1.90	96.4	93.4	5.3	14257	0.35
$\lambda 2$ (1.0724)	2.00	97.3	98.5	5.5	22957	0.39
$\lambda 3$ (1.0744)	2.00	97.6	100.0	5.9	12337	0.39
$\lambda 4$ (1.0543)	2.00	98.1	100.0	6.0	22977	0.39
bromide						
$\lambda 1$ (0.9180)	1.66	77.9	69.4	6.5	16961	0.73
$\lambda 2$ (0.9160)	1.66	78.3	72.9	8.6	16875	0.71
$\lambda 3$ (0.8856)	1.61	76.8	79.2	7.5	18503	0.75
$\lambda 4$ (0.9552)	1.73	79.1	63.0	4.7	15349	0.73
xenon						
λ (1.54)	1.79	75.8	13.9	4.4	13149	0.68
native						
λ (1.00)	1.20	92.2	63.3	4.3	53030	0.53

MAD/MIR Results

derivative	no. of sites	phasing power[b] centric	phasing power[b] acentric
platinum	1	0.87	0.18
bromide	9	0.78	0.36
xenon	2	0.35	0.35

Figure of Merit (25−2.5 Å)

acentric reflections	centric reflections	all reflections
0.57	0.41	0.56

[a] $R_{sym} = \Sigma|I_h - \langle I_h \rangle|/\Sigma|I_h|$. [b] Phasing power = $\Sigma|F_{Hcalc}|/\Sigma|(F_P + F_{Hcalc}) - F_{PH}|$.

f' ($\lambda 2$) and maximum f'' ($\lambda 4$) were determined by X-ray fluorescence spectra. Single wavelength data for the native protein and the Xe derivative were collected at 1 and 1.54 Å, respectively. All data were processed and scaled with HKL2000 (Table 1) (*17*). Initial phases were obtained using 20.0−2.5 Å resolution data from three experiments: Pt MAD, Br^- MAD, and Xe single wavelength anomalous dispersion. Heavy atom localization and phasing calculations were carried out with the standard scripts in the program SOLVE (*18*). A total of 12 heavy atoms/anomalous scatters (1 Pt, 9 Br^-, and 2 Xe) were included in Patterson correlation refinement. The electron density was improved though the maximum likelihood density modification algorithm as implemented in RESOLVE (*19*, *20*). Initial maps were calculated with the CCP4 programs suite (*21*). The resulting map showed most of the main chain structure along with some side chain electron density allowing for the construction of approximately 90% of the final model. Subsequent model building and refinement was performed with Turbo Frodo and CNS, respectively (*22*, *23*). Intermediate structures were compared to SIGMAA-weighted $2F_o - F_c$ and $F_o - F_c$ electron density maps and revised accordingly (*24*). The partial model was then refined against the native data set, which is 92.2% complete with an average $I/\sigma = 29.6$ (63.3% complete with an average $I/\sigma = 1.6$ in the last shell). The progress of refinement was monitored by a decrease in both R_{cryst} and R_{free} at each stage of simulated annealing, energy minimization, and individual isotropic B-factor refinement. The resolution of the electron density maps was extended incrementally during each round of refinement and manual rebuilding, reaching 1.2 Å in the final round. The final model contains 185 water molecules and one citrate anion and

Table 2: Refinement Statistics

R_{free} (%)	21.9
$R_{working}$ (%)	22.7
avg B factor for all atoms (Å^2)	15.0
avg B factor for main chain atoms (Å^2)	12.5
avg B factor for side chain (Å^2)	13.8
avg B factor for solvent (Å^2)	22.9
avg B factor for citrate ion (Å^2)	23.6
rmsd bond length (Å)	0.004
rmsd angles (°)	1.1
no. of protein atoms	1276
no. of water molecules	185
no. of citrate ions	1
Ramachandron Plot	
residues in most favored regions	126 (88.7%)
residues in additionally allowed regions	15 (10.6%)
residues in generously allowed regions	0
residues in disallowed regions	1 (0.7%)[a]

[a] The conformation of this residue, Tyr 112, is correct due to its unambiguous fit to the electron density.

yielded an R_{cryst} = 21.9% and R_{free} = 22.8% (Table 2). Geometry of the final model was evaluated with PROCHECK (*25*) and showed 88.7% of the residues in the most favored conformation. 10.6% of the residues are located in additionally allowed regions while one residue (Tyr 112) is located in a disallowed region. Inspection of both $2F_o - F_c$ and $F_o - F_c$ electron density maps in this region revealed that this residue fits well to the electron density and that its unusual conformation is correct.

An additional set of data was collected for crystals soaked in the crystallization solution adjusted to pH 7.0. The structure was refined at a resolution of 1.9 Å to an R = 23.9% and R_{free} = 25.5%. No major structural differences were observed between the two models except for the absence of the bound citrate ion at the opening of the calyx. A superposition of C_α atoms resulted in an rms deviation of 0.57 Å and showed no major pH-dependent loop shifts.

C8α Peptide Binding. A synthetic peptide containing the sequence found at the putative C8γ binding site in C8α (GELRYDSTGERLYYGDDEKY) was prepared as described elsewhere (*26*). This sequence corresponds to C8α residues 157−175 and has been modified by addition of an N-terminal Gly and a Cys^{164} → Gly^{164} substitution. For crystal soaking, the peptide was solubilized in 0.36 M sodium citrate, pH 4.0, at room temperature. This solution was then adjusted with 50% PEG 4000 to create an artificial mother liquor containing the peptide, 36% PEG, and 0.1 M sodium citrate, pH 4.0. A single crystal of C8γ was introduced into a drop containing the artificial mother liquor and allowed to equilibrate for one month. Data were collected under cryo conditions employing a Rigaku rotating anode source at 50 kV and 100 mA with Yale mirror optics and an R-Axis IV area detector at a distance of 100 mm. Data were processed with HKL2000; however, after rejection of reflections with $I < 1\sigma(I)$, the data set was only 76.3% complete to 1.77 Å resolution (79.3% in the 1.84−1.77 shell) with 13 618 unique reflections and R_{merge} = 6.2%.

RESULTS

Quality of the Model. Figure 1 illustrates the quality of the electron density maps, which allowed for the unambiguous placement of nearly all 182 amino acids in C8γ.

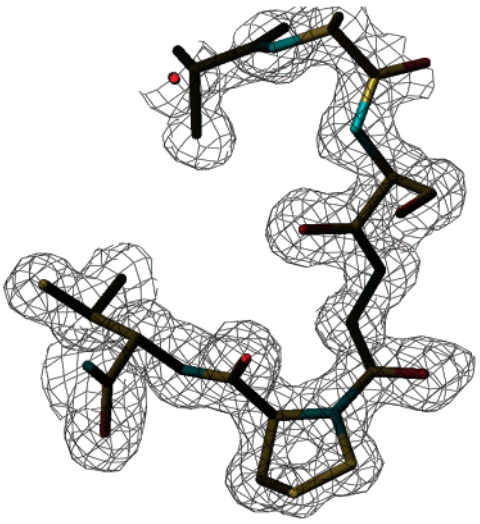

FIGURE 1: A representative portion of the C8γ electron density map at 1.2 Å resolution contoured at 1σ. Density shows holes in all five- and six-membered rings, allowing for the refinement of kinked prolines.

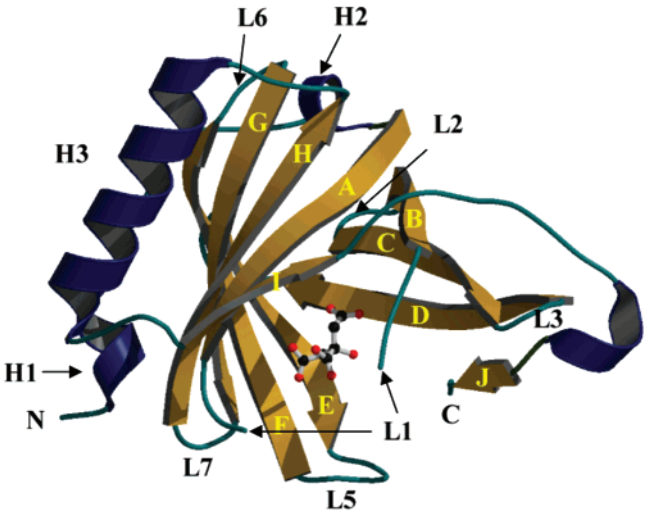

FIGURE 2: Ribbon diagram of the C8γ structure. β-strands are shown in yellow (A−J) and helices in blue (H1−H3). H1 (S11−S14) and H2 (A24−F27) are 3_{10}-helices, whereas H3 is an α-helix (D139−E151). Loop regions are designated L1-L7. L1 lies between strand A (G29−G37) and B (T53−Q60); however, due to its disorder only part of the loop is shown. L2 lies between B and C (A63−L72), L3 lies between C and D (I75−D85), and L4, which cannot be seen in this view because it falls behind the structure, lies between D and E (R91−R94). L5 lies between E and F (V103−T110), L6 lies between F and G (F115−R122), and L7 lies between G and H (Q125−A132). Helix H3 lies between strand H and I (I159−Y161); strand I is joined to J (V176−D178) by a random coil. A citrate molecule from the crystallization buffer is shown at the opening of the calyx.

Exceptions include the first nine N-terminal residues and two C-terminal residues, which were disordered, residues F42−H48 that comprise a disordered portion of a loop spanning the open end of the calyx (loop 1), and the side chain atoms of R41, R49, and R97−R100, which were not well defined in the $2F_o - F_c$ density map. Also, the side chains of S134, S140, Q150, and F162 displayed two alternative conformations.

Overall Structure. C8γ displays a typical lipocalin fold that consists of an eight-stranded continuously hydrogen bonded β-barrel with an additional ninth and tenth β-strand

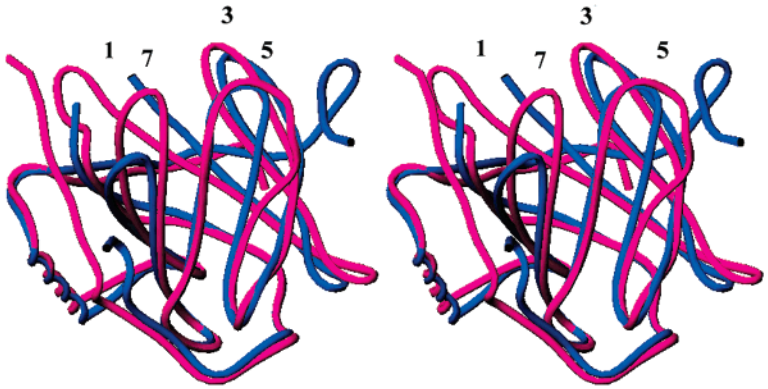

FIGURE 3: Stereoview of NGAL (magenta) superimposed on C8γ (blue). Loops are numbered as they occur in the primary structure. Loop 1 (N39−Y52 in NGAL and S38−A52 in C8γ) is shown as incomplete for C8γ because of disorder in residues F42−H48. Loop 7 (R128−Y132 in NGAL and A123−G124 in C8γ) extends further upward in NGAL as compared to C8γ. Loops 3 and 5 in C8γ are also shifted with respect to NGAL. Loop 3 (K73−K74 in NGAL and D73−G74 in C8γ) is shifted ~3 Å away from the calyx, whereas loop 5 (G95−G102 in NGAL and Q95−A102 in C8γ) is shifted ~5 Å in toward the calyx leading to a slight overall narrowing of the binding site.

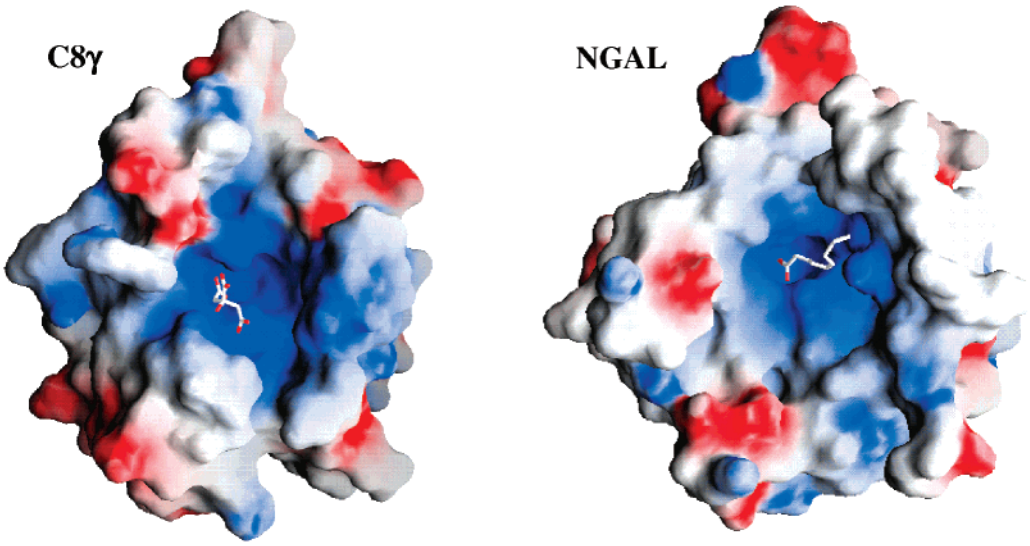

FIGURE 4: Molecular surfaces of C8γ and NGAL colored according to electrostatic potential. Positive charge is in blue and negative charge in red. Both molecules are in approximately the same orientation to allow for viewing into the calyces. Ligands are rendered in as rods with carbons in white and oxygens in red. NGAL is shown with a copurified free fatty acid that only partially fills the binding site (*27*) and C8γ is shown with citrate bound at the opening of the calyx. The binding site of NGAL is slightly wider than that of C8γ, while C8γ's binding pocket is deeper. Figure generated by the program GRASP (*31*).

completing the barrel (Figure 2). The structure contains a short 3_{10} helix at the N-terminus, a second 3_{10} helix that packs across a conserved tryptophan (W31) at the closed end of the barrel, and an α-helix that flanks the calyx. Loop 1, which restricts access to the binding site in some lipocalins, is disordered and presumably exhibits considerable conformational variation. Cys^{40}, which forms the disulfide bond to C8α, is located in this loop.

Compared to other lipocalins whose structures are known, C8γ is most structurally similar to human NGAL (PDB entry 1QQS) (*27*). Superposition of the NGAL and C8γ secondary structures yields a match rate of 74.7% and an rms deviation between C_α atoms of 1.35 Å for matching residues (*28*). Interestingly, C8γ shares only 19.4% sequence identity with NGAL. The well-characterized human retinol binding protein RBP shares a higher sequence identity (27.8%) but superimposes on C8γ with a structural similarity match rate of only 69.3% (rms = 1.45 Å) (PDB entry 1FEM) (*29*, *30*). Such disparity between sequence identity and structural similarity is common among lipocalins.

The backbone of NGAL superimposes well on C8γ with the most deviation occurring in the loop regions at the opening of the calyx (Figure 3). The C8γ calyx is quite similar to that of NGAL as it is fairly wide with hydrophilic, positively charged residues near the opening (Figure 4). However, it is much deeper than that of NGAL. The apparent base of NGAL's binding pocket is formed by residues F83, Y138, F123, and Y56, which fill the deepest portion of the calyx. In C8γ, the corresponding residues are Y83, Y131, L120, and V57. The smaller side chains of L120 and V57 create a hydrophobic cavity at the bottom of the calyx with an opening of sufficient size to allow penetration of a single hydrocarbon chain.

Experimental evidence indicates the cavity itself could accommodate a larger moiety. Strong density corresponding to two Xe atoms, and a third weaker peak, was observed within this pocket (data not shown). The relatively large Xe atom has been used as a probe to study cavities and hydrophobic sites in several proteins (*32*). Such regions are usually devoid of ordered water molecules and normally

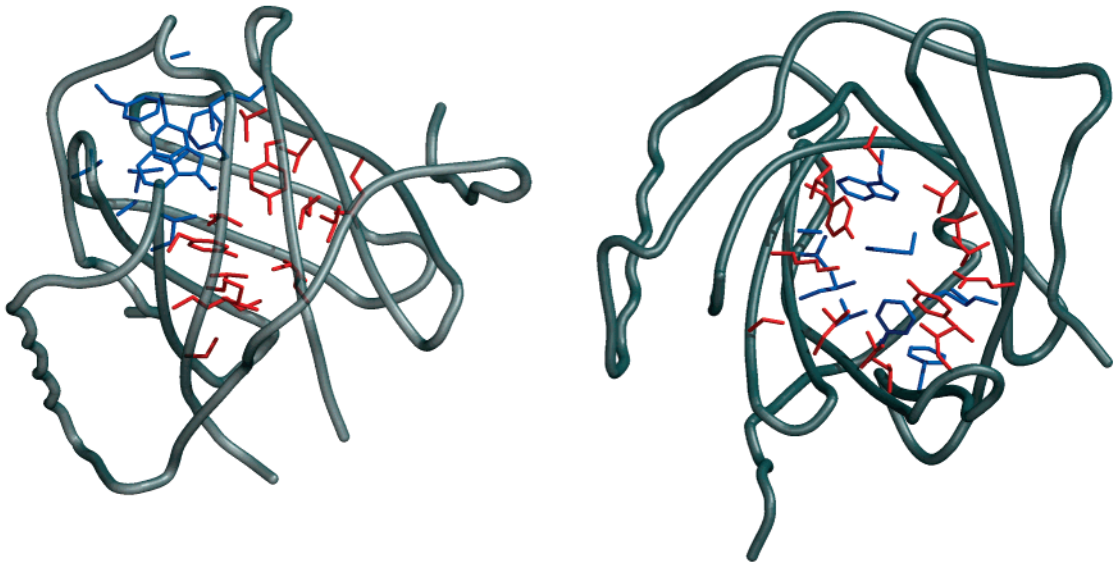

FIGURE 5: Molscript rendering of C8γ showing the residues lining the hydrophobic (blue) and hydrophilic (red) portions of the binding pocket. Left: Side view of the C8γ calyx. Right: View looking directly into the mouth of the calyx. Residues lining the bottom of the calyx are F22, A24, F27, W31, M64, F92, V107, T110, A116, and L118. Residues lining the middle portion of the calyx are L33, L55, V57, V66, T68, Q81, Y83, L94, V103, V105, L120, S127, K129, and Y131.

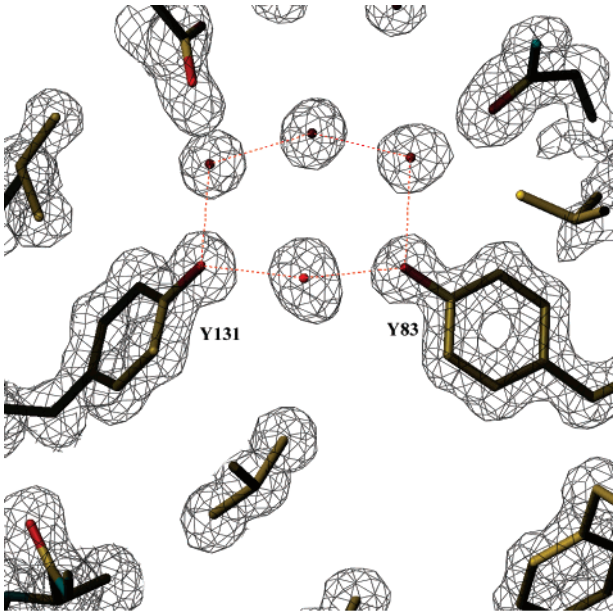

FIGURE 6: Side view of the middle portion of the binding pocket in C8γ. Y83 and Y131 appear to form a gate to the deep hydrophobic region of the calyx. Above the gate and out of view is the positively charged entrance to the calyx, while a portion of the hydrophobic pocket can be seen below the gate. Also out of view are residues L120 and V57, which by virtue of their smaller side chains provide space for ligand access to this lower pocket. The tyrosine hydroxyls are hydrogen-bonded to four water molecules to form a hexagonal arrangement that separates the hydrophilic and hydrophobic portion of the binding pocket. This suggests the natural ligand possesses some hydrogen bond acceptors adjacent to the hydrophobic portion of its structure.

accommodate a single Xe atom. In agreement with these generalizations, the deepest portion of the C8γ calyx is hydrophobic and devoid of ordered water, yet it is much larger (with a volume of about 100 Å^3) than a typical protein cavity (Figure 5). The side chains of Y83 and Y131 appear to partially restrict access to the bottom portion of the calyx and may act as a gate (Figure 6). If indeed a moiety larger than a single hydrocarbon chain enters the bottom portion of the calyx, conformational changes in these residues would be necessary to provide access.

Citrate Binding. Well-resolved density corresponding to a citrate ion from the crystallization buffer is observed within hydrogen bonding distance from the ϵ-NH_3^+ group of K129 at the opening of the calyx (Figure 7). The citrate ion is anchored by this lysine and stabilized through additional hydrogen bonds to the guanidinium group of R70 and three water molecules. Within the vicinity of the citrate ion and ringing the entrance to the calyx are several positively charged residues, namely, R41, R49, R70, R100, and R122. This suggests that the natural ligand for C8γ contains anionic moieties such as carboxylate or phosphate groups at one end. Interestingly, no citrate ion binding was observed at pH 7.0 where the ion has an overall charge of -3 as compared to -2 at pH 4.0.

Binding of the C8α *Indel Peptide*. Crystals soaked with a synthetic peptide containing sequence found at the putative C8γ binding site in C8α exhibited additional electron density corresponding to three amino acid residues (data not shown). The location of this density was near loop 1 and overlapped with the citrate ion binding site in the native structure. This peptide contains three negatively charged aspartic residues, two of which are adjacent to each other and could possibly be involved in binding to positively charged residues near the opening of the calyx. However, the overall quality of the diffraction data was only moderate, and these residues could not be fitted to the electron density with certainty. Additionally, loop 1 maintained its disordered state, and thus no information on the conformation of loop 1 in the peptide–C8γ complex could be extracted from the data.

DISCUSSION

This report describes the first three-dimensional structure of a protein component of the MAC. C8γ displays a typical lipocalin fold, thus confirming predictions based on its amino acid sequence and genomic structure. Its structure is most similar to human NGAL, a lipocalin released from granules

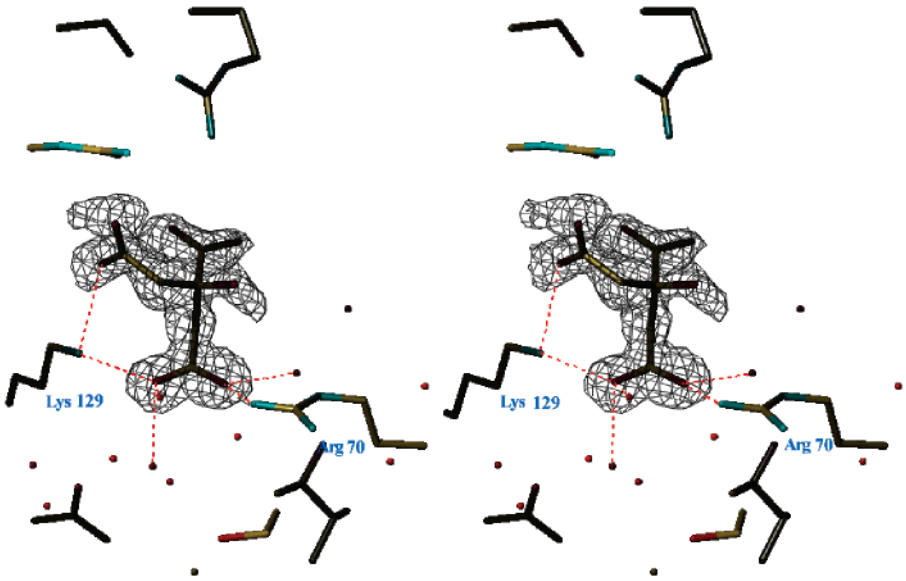

FIGURE 7: A citrate ion modeled into $2F_o - F_c$ density contoured at 1σ. K129 coordinates two carboxylase groups of the citrate ion, while R70 and three water molecules are also within hydrogen bonding distance from the ion. Within the vicinity of the citrate and ringing the entrance to the calyx are several other arginines and lysines (not shown) that may serve to coordinate anionic moieties such as carboxyl or phosphate groups.

of activated neutrophils (*33*, *34*). Although the function of NGAL is unknown, it is thought to have a role in modulating the inflammatory response by binding and neutralizing bacterial products or other proinflammatory small molecules released at the site of an infection. C8γ is structurally similar to NGAL in that it forms a calyx with a relatively large hydrophilic entry that carries an overall positive charge. However, unlike NGAL, C8γ has a deep hydrophobic cavity that is accessible through a somewhat constricted, hydrophilic portion of the binding pocket. This suggests the C8γ ligand is longer and thinner than the NGAL ligand.

The functional significance of the ligand binding site in C8γ is unclear. It was originally proposed that such a site may mediate binding to C8α. When the MAC assembles on target cells, C8α inserts into the membrane bilayer (*5*); therefore, it must contain one or more hydrophobic regions with the potential to bind lipid. It was suggested that C8γ may bind to such a region and shield C8α from premature membrane interactions, either during biosynthetic processing or while in the circulation (*35*). Subsequent studies showed that C8α can be produced independently as a recombinant protein; therefore, such a role for C8γ is now considered less likely (*16*). Results from the present study support this conclusion. The binding pocket in C8γ is much wider and deeper than necessary to accommodate a single amino acid side chain as the ligand. The mouth of the calyx is sufficiently wide to accommodate multiple side chains associated with a loop; however, little penetration into the calyx interior could occur. Thus, it seems unlikely the ligand binding site serves as the principal mediator of C8α binding.

The site of interaction with C8α most likely resides in or near loop 1, which is relatively large and contains Cys^{40}. During intracellular processing, C8α and C8γ must associate prior to formation of the disulfide bond in C8$\alpha-\gamma$; therefore, they must contain complementary binding sites for each other. This is supported by in vitro studies using purified C8α and C8γ (*7*). In C8α, the binding site for C8γ has been localized to a unique 17-residue insertion (indel) at position 159−175 (*26*). This segment includes Cys^{164} that forms the disulfide bond to Cys^{40} in C8γ. Importantly, a synthetic peptide containing this sequence was coupled to agarose and shown to specifically bind C8γ. In the present study, crystals soaked with this peptide revealed additional electron density near loop 1, thus supporting the prediction that this region of C8γ is involved in binding C8α. Loop 1 is disordered at both low and neutral pH as well as in the presence of the indel peptide, which suggests conformational flexibility in this region. It may be that during assembly of the MAC, conformational changes in C8α influence the position of loop 1 and this in turn controls access to the ligand binding site.

At the present time, one can only speculate on the identity of the natural ligand for C8γ. Crystallographic analyses revealed no associated ligand other than a citrate ion from the crystallization buffer. Mass spectral analysis likewise revealed no endogenous ligand bound to purified recombinant C8γ.[2] Several lipocalins are capable of binding retinoids; however, in most cases binding is nonspecific, and the functional significance is not obvious (*36*). Binding of radiolabeled retinol and retinoic acid to C8$\alpha-\gamma$ has been reported, and it was suggested that C8γ is a retinol transport protein (*37*). However, these results could not be corroborated in studies using purified C8γ and spectroscopic methods to detect retinol binding (*16*).

Analysis of the C8γ structure superimposed on that of a RBP−retinoic acid complex supports the latter findings. The overall shape, size, and charge of the binding pocket is not conducive to retinoid binding. The binding pocket in C8γ is nearly twice as wide at the mouth of the calyx than that of RBP (18 vs 9 Å). A major contribution to the widening of the calyx can be attributed to the observation that C8γ contains an extra β-strand (residues V176−D178) that serves to enlarge the diameter of the calyx. Additionally, a shift in β-strands A and H in C8γ away from the center of the calyx further widens the binding pocket. Thus, C8γ lacks the ability

[2] Parker, C. L., and Sodetz, J. M., unpublished results.

to make sufficient hydrophobic contacts with much of the aliphatic chain of retinoic acid. There is also a major difference in the loop structures. Loop 1 in RBP is smaller and extends across the mouth of the calyx to stabilize retinoic acid. The corresponding loop in C8γ is partially disordered; however, it appears to protrude away from the center of the calyx. Loop 3 in RBP is much longer and along with loop 5 is shifted toward the center of the calyx to further stabilize bound retinoic acid. Residues lining the binding pockets of these proteins are also significantly different (*30*). The hydrophobic residues responsible for stabilizing the bulky, hydrophobic six-membered ring of retinoic acid in RBP (F97 and F137) are replaced by the more hydrophilic residues Y83 and Y131 in C8γ. Also, the upper portion of the pocket in C8γ is hydrophilic and carries an overall positive charge, whereas the binding cavity in RBP is somewhat hydrophilic but remains essentially neutral.

The characteristics of the binding pocket are suggestive of a fatty acid or related compound as the ligand for C8γ. The depth and shape can accommodate an elongated hydrophobic structure such as the aliphatic portion of a fatty acid with a chain length up to C_{12}. The contour of the pocket is also compatible with a single monounsaturated fatty acid. Positively charged residues around the opening of the calyx suggest the ligand has negative charge(s) at one end.

One obvious source of a fatty acid-related ligand is the membrane upon which the MAC is formed, e.g., glycerophospholipid from mammalian membranes or lipid A from the lipopolysaccharide of gram-negative bacteria. Exposure of membrane lipid during assembly of the MAC may render fatty acid side chains accessible to C8γ. Such a binding function has not been considered previously because C8γ was thought to be located on the periphery of the MAC and away from the membrane (*5*, *7*). Moreover, C8γ is not required for MAC-mediated lysis of membranes. A complex of C8α and C8β is an effective substitute for C8 in lysing simple cells such as erythrocytes (*16*, *38*) and in killing gram-negative bacteria.[2] However, the activity of this complex is lower relative to C8, which indicates that C8γ functions in some manner to enhance MAC activity. The results here suggest binding of C8γ to membrane-associated fatty acids may be one mechanism by which this occurs.

Without a clear understanding of its role in the complement system, it is difficult to speculate on the identity of a soluble ligand for C8γ. The MAC deposits on the outer membrane of gram-negative bacteria; therefore, C8γ is exposed to a variety of inflammatory mediators produced at the site of an infection. One intriguing possibility is that it binds to a small hydrophobic mediator and modulates the local inflammatory response as suggested for NGAL. An alternative possibility is that C8γ transports an as yet unidentified ligand in the circulation. Experiments investigating both these possibilities and the potential for C8γ to bind to membrane-associated lipids are in progress.

REFERENCES

1. Esser, A. F. (1994) The membrane attack complex of complement: assembly, structure and cytotoxic activity. *Toxicology 87*, 229−247.
2. Plumb, M. E., and Sodetz, J. M. (1998) Proteins of the membrane attack complex, in *The Human Complement System in Health and Disease* (Volanakis, J. E., and Frank, M. M., Eds.) pp 119−148, Marcel Dekker, New York.
3. Ng, S. C., Rao, A. G., Howard, O. M., and Sodetz, J. M. (1987) The eighth component of human complement (C8): evidence that it is an oligomeric serum protein assembled from products of three different genes. *Biochemistry 26*, 5229−5233.
4. Monahan, J. B., and Sodetz, J. M. (1981) Role of the beta subunit in interaction of the eighth component of human complement with the membrane-bound cytolytic complex. *J. Biol. Chem. 256*, 3258−3262.
5. Steckel, E. W., Welbaum, B. E., and Sodetz, J. M. (1983) Evidence of direct insertion of terminal complement proteins into cell membrane bilayers during cytolysis: labeling by a photosensitive membrane probe reveals a major role for the eighth and ninth components. *J. Biol. Chem. 258*, 4318−4324.
6. Stewart, J. L., and Sodetz, J. M. (1985) Analysis of the specific association of the eighth and ninth components of human complement: identification of a direct role for the α subunit of C8. *Biochemistry 24*, 4598−4602.
7. Brickner, A., and Sodetz, J. M. (1985) Functional domains of the α-subunit of the eighth component of human complement: identification and characterization of a distinct binding site for the γ chain. *Biochemistry 24*, 4603−4607.
8. Lockert, D. H., Kaufman, K. M., Chang, C. P., Hüsler, T., Sodetz, J. M., and Sims, P. J. (1995) Identity of the segment of human complement C8 recognized by complement regulatory protein CD59. *J. Biol. Chem. 270*, 19723−19728.
9. Plumb, M. E., Scibek, J. J., Barber, T. D., Dunlap, R. J., Platteborze, P. L., and Sodetz, J. M. (1999) Chimeric and truncated forms of human complement protein C8α reveal binding sites for C8β and C8γ within the membrane attack complex/perforin region. *Biochemistry 38*, 8478−8484.
10. Schreck, S. F., Parker, C., Plumb, M. E., and Sodetz, J. M. (2000) Human complement protein C8γ, *Biochim. Biophys. Acta 1482*, 199−208.
11. Haefliger, J. A., Jenne, D., Stanley, K. K., and Tschopp, J. (1987) Structural homology of human complement component C8γ and plasma protein HC: identity of the cysteine bond pattern. *Biochem. Biophys. Res. Commun. 149*, 750−754.
12. Kaufman, K. M., and Sodetz, J. M. (1994) Genomic structure of the human complement protein C8γ: homology to the lipocalin gene family. *Biochemistry 33*, 5162−5166.
13. Flower, D. R. (1996) The lipocalin protein family: structure and function. *Biochem. J. 318*, 1−14.
14. Flower, D. R., North, C. T., and Sansom, C. E. (2000) The lipocalin protein family: structural and sequence overview. *Biochim. Biophys. Acta 1482*, 9−24.
15. Flower, D. R. (2000) Experimentally determined lipocalin structures. *Biochim. Biophys. Acta 1482*, 46−56.
16. Schreck, S. F., Plumb, M. E., Platteborze, P. L., Kaufman, K. M., Michelotti, G. M., Letson, C. S., and Sodetz, J. M. (1998) Expression and characterization of recombinant subunits of human complement component C8: further analysis of the function of C8α and C8γ. *J. Immunol. 161*, 311−318.
17. Otwinowski, Z., and Minor, W. (1997) Processing of X-ray diffraction data collected in oscillation mode. *Methods Enzymol. 276*, 307−326.
18. Terwilliger, T. C., and Berendzen, J. (1999) Automated structure solution for MIR and MAD. *Acta Crystallogr. D55*, 849−861.
19. Terwilliger, T. C. (1999) Reciprocal-space solvent flattening. *Acta Crystallogr. D55*, 1863−1871.
20. Terwilliger, T. C. (2000) Maximum likelihood density modifications. *Acta Crystallogr. D56*, 965−972.
21. Collaborative Computing Project, Number 4. (1994) The CCP4 suite: programs for protein crystallography. *Acta Crystallogr. D50*, 760−763.
22. Russel, A., Cambillau, C. (1991) "Turbo Frodo" Silicon Graphics Geometry Partners Directory. Mountain View, CA, Silicon Graphics, 86.
23. Brunger, A. T., Adams, P. D., Clore, G. M., Delano, W. L., Gros, P., Grosse-Kunstleve, Reed, R. J., Jiang, J., Kuszewskic, J., Nilges, M., Pannu, N., Read, R. J., Rice, L. M., Simonson, T., and Warren, G. L. (1998) Crystallography & NMR System: A new software suite for macromolecular structure determination. *Acta Crystallogr. D54*, 905−921.

24. Reed, R. J. (1986) Improved Fourier coefficients for maps using phases from partial structures with errors. *Acta Crystallogr. A42*, 140−149.
25. Laskowski, R. A., MacArthur, M. W., Hutchinson, E. G., and Thornton, J. M. (1992) *PROCHECK*: a program to check the stereochemical quality of protein structures. *J. Appl. Crystallogr. 26*, 283−291.
26. Plumb, M. E., and Sodetz, J. M. (2000) An indel within the C8α subunit of human complement C8 mediates intracellular binding of C8γ and formation of C8$\alpha-\gamma$. *Biochemistry 39*, 13078−13083.
27. Goetz, D. H., Willie. S. T., Armen, R. S., Bratt, T., Borregaard, N., and Strong, R. K. (2000) Ligand preference inferred from the structure of neutrophil gelatinase associated lipocalin. *Biochemistry 39*, 1935−1941.
28. Lu, G. (2000) TOP: A new method for protein structure comparisons and similarity searches. *J. Appl. Crystallogr. 33*, 176−183.
29. Newcomer, M. E., and Ong, D. E. (2000) Plasma retinol binding protein: structure and function of the prototypic lipocalin. *Biochim. Biophys. Acta 1482*, 57−64.
30. Zanotti, G., Marcello, M., Malpeli, G., Folli, C., Sartori, G., and Berni, R. (1994) Crystallographic studies on complexes between retinoids and plasma retinol-binding protein. *J. Biol. Chem. 269*, 29613−29620.
31. Nicholls, A., Sharp, K. A., and Honig, B. (1991) Protein folding and association: insights from the interfacial thermodynamic properties of hydrocarbons. *Proteins 11*, 281−296.
32. Prange, T., Schiltz, M., Pernot, L., Colloc, N., Longhi, S., Bourguet W., and Fourme, R. (1998) Exploring hydrophobic sites in proteins with xenon or krypton. *Proteins 30*, 61−73.
33. Kjeldsen, L., Bainton, D. F., Sengeløv, H., and Borregaard, N. (1994) Identification of neutrophil gelatinase-associated lipocalin as a novel matrix protein of specific granules in human neutrophils. *Blood 83*, 799−807.
34. Kjeldsen, L., Cowland, J. B., and Borregaard N. (2000) Human neutrophil gelatinase-associated lipocalin and homologous proteins in rat and mouse. *Biochim. Biophys. Acta 1482*, 272−283.
35. Sodetz, J. M. (1989) Structure and function of C8 in the membrane attack sequence of complement. *Curr. Top. Microbiol. Immunol. 140*, 19−31.
36. Åkerstrom, B., Flower, D. R., and Salier, J−P. (2000) Lipocalins: unity in diversity. *Biochim. Biophys. Acta 1482*, 1−8.
37. Haefliger, J. A., Peitsch, M. C., Jenne, D. E., and Tschopp, J. (1991) Structural and functional characterization of complement C8γ, a member of the lipocalin protein family. *Mol. Immunol. 28*, 123−131.
38. Brickner, A., and Sodetz, J. M. (1984) Function of subunits within the eighth component of human complement: selective removal of the γ chain reveals it has no direct role in cytolysis. *Biochemistry 23*, 832−837.

BI025696I